Effects of New Cage Profiles on the Improvement in Biomechanical Performance of Multilevel Anterior Cervical Corpectomy and Fusion: A Finite Element Analysis

Ning Liu[1,2], Teng Lu[1,3], Yibin Wang[1], Zhongwei Sun[4], Jialiang Li[1], Xijing He[1]

■ BACKGROUND: **For multilevel cervical fusion, anterior corpectomy and fusion (ACCF) induces more implant-related complications than anterior diskectomy and fusion (ACDF), which implies that the biomechanical stability of ACCF may be insufficient. The aim of this study was to assess whether the optimization of the cage profiles could improve the biomechanical performance of multilevel ACCF.**

■ METHODS: **Three finite element models were constructed and compared, including 3-level ACDF, 2-level ACCF using a conventional cage for reconstruction, and 2-level ACCF using a new cage for reconstruction. The ends of the new cage possessed additional end rings and emulated the end plate geometries. The ranges of motion (ROMs) of the surgical segments and the stress peaks in the end plate, fixation system, and screw-bone interface were compared.**

■ RESULTS: **Compared with preoperative status, ACDF and ACCF reduced the segmental ROMs by 96.1%—98.2%. The end plate stress peaks were the highest in ACCF using the conventional cage (10.1—18.6 MPa), followed by ACCF using the new cage (7.7—14.3 MPa) and ACDF (5.3—9.1 MPa). ACDF induced the highest stress peaks in the fixation system and screw-bone interface (32.5—39.3 MPa and 12.1—12.7 MPa, respectively), followed by ACCF using the conventional cage (20.4—31.7 MPa and 10.3—13.6 MPa, respectively) and ACCF using the new cage (18.6—25.7 MPa and 9.7—12.6 MPa, respectively).**

■ CONCLUSIONS: **The application of the new cage decreased the risks of cage subsidence and instrument-related complications in multilevel ACCF. Under the condition where cage subsidence was prevented, ACCF was superior to ACDF in terms of construct stability and avoiding instrument-related complications.**

INTRODUCTION

Cervical spondylotic myelopathy (CSM) is a common degenerative disease that induces spinal cord compression and dysfunction in older people.[1] The primary treatment for CSM is to decompress the spinal cord and prevent the progression of neurologic symptoms.[2,3] Anterior cervical diskectomy and fusion (ACDF) and anterior cervical corpectomy and fusion (ACCF) are the 2 most commonly used surgical procedures for the treatment of multilevel CSM.[4,5] Although both techniques have been shown to be effective,[6,7] there is not a consensus on the superiority of ACDF or ACCF.[5,8] ACCF has larger visual exposure for the operation and allows for more extensive decompression than ACDF.[9,10] However, ACDF is less difficult to perform and has a lower risk of excessive bleeding and neurologic injury; therefore, this procedure may be safer for elderly patients and those with other comorbidities.[6,7] In addition, ACCF induces a much higher

Key words
- Cage design
- Cage subsidence
- Cervical
- Corpectomy
- Diskectomy
- Finite element
- Fusion

Abbreviations and Acronyms
ACCF: Anterior cervical corpectomy and fusion
ACDF: Anterior cervical diskectomy and fusion
CSM: Cervical spondylotic myelopathy
CT: Computed tomography
FE: Finite element
ROM: Range of motion

From the [1]Department of Orthopedics, Second Affiliated Hospital of Xi'an Jiaotong University, Xi'an, Shaanxi Province, China; [2]Department of Spine Surgery, Hanzhong Central Hospital, Hanzhong, Shaanxi Province, China; [3]Department of Neurosurgery, Brigham and Women's Hospital, Harvard Medical School, Boston, Massachusetts, USA; and [4]Department of Research and Development, ZSFab, Inc., Boston, Massachusetts, USA

To whom correspondence should be addressed: Xijing He, M.D., Ph.D.
[E-mail: he_xijing@126.com]

Citation: World Neurosurg. (2019) 129:e87-e96.
https://doi.org/10.1016/j.wneu.2019.05.037

*Journal homepage: **www.journals.elsevier.com/world-neurosurgery***

*Available online: **www.sciencedirect.com***

incidence of implant-related complications than ACDF,[11,12] which implies that the biomechanical stability of a multilevel ACCF construct may be insufficient.

Cage subsidence is an initial sign of biomechanical instability in ACCF because this subsidence subsequently impairs the construct immobilization and increases the stresses on the anterior fixation system, which increases the risks of instrument-related complications, such as fixation looseness, breakage, and extrusion.[13-15] Recently, some new cages that are designed with enlarged ends and are aligned with the end plate geometries have been used for vertebral body reconstruction in single-level ACCF.[16-18] Postoperative outcomes have shown that the subsidence rate when using the new cage was effectively less than that using the conventional cage.[16-18] However, evidence of the biomechanical benefits of using the cage with the new profiles for multilevel ACCF has been limited. The aims of our study are 1) to assess whether the biomechanical performance in multilevel ACCF can be improved by using the new cage that possessed additional end rings and emulated the end plate geometries, and 2) to assess the differences in biomechanical performances between multilevel ACCF and ACDF.

MATERIALS AND METHODS

Finite Element Modeling of the Intact Lower Cervical Spine

A nonlinear intact C3-7 finite element (FE) model was constructed with the following steps. Computed tomography (CT) images of the C3-7 cervical spine were obtained from a young healthy volunteer (29 years of age; height, 174 cm; weight, 78 kg) and were then imported into Mimics (Materialise Inc., Leuven, Belgium) to reconstruct the surface model of each vertebra. Solid models of the cortical shell, cancellous bone, and intervertebral disk were constructed in 3-Matic (Materialise Inc.). Mesh models of the bones, intervertebral disks, and ligaments were constructed using HyperMesh (Altair Engineering, Inc., Troy, Michigan, USA) and imported into Abaqus (Hibbitt, Karlsson and Sorenson, Inc., Providence, Rhode Island, USA) for material property definitions, model assembly, and FE analysis.

Figure 1 shows the FE model of the intact C3-7 cervical spine, which consisted of 5 vertebrae, 4 intervertebral disks, the anterior longitudinal ligament, the posterior longitudinal ligament, the capsular ligament, the interspinous ligament, and the ligamentum flavum. The thickness of the cortical shell was defined as 1 mm. The nucleus pulposus was modeled as an incompressible fluid, and the volume of the nucleus pulposus accounted for 30%—40% of the intervertebral disk.[19] The annulus fibrosus was modeled as an annulus ground substance embedded with annulus fibers. The fibers were modeled as truss elements and were positioned at an inclination of $\pm 25°-35°$ from the transverse plane.[19,20] The ligaments were modeled as truss elements that respond nonlinearly in tension only. Hypoelastic material properties were assigned to the ligament according to the stress-strain curves that were published previously.[19] A convergence analysis was performed to ensure that the maximum changes in the strain energy were $<5\%$. The element types and material properties used in the FE model were defined based on previous publications[19,21] and are shown in Table 1 and Figure 2.

FE Modeling of the ACDF and ACCF Procedures

Figures 3A—D show the FE models of ACDF at C4-7. The diskectomies were simulated by removing the C4-5, C5-6, and C6-7 intervertebral disks and the corresponding anterior and posterior longitudinal ligaments. After decompression, a suitably sized polyetheretherketone interbody cage ($5 \times 11 \times 11$ mm) (Compact CORNERSTONE-SR [Medtronic Inc., Memphis, Tennessee, USA]) was modeled and inserted into the intervertebral spaces to simulate the interbody fusion. Both ends of the cage were ensured to be in complete contact with the corresponding end plates. The contact area in the cage—end plate interface end was 0.64 cm^2. An anterior plate-screw system was placed at C4-7

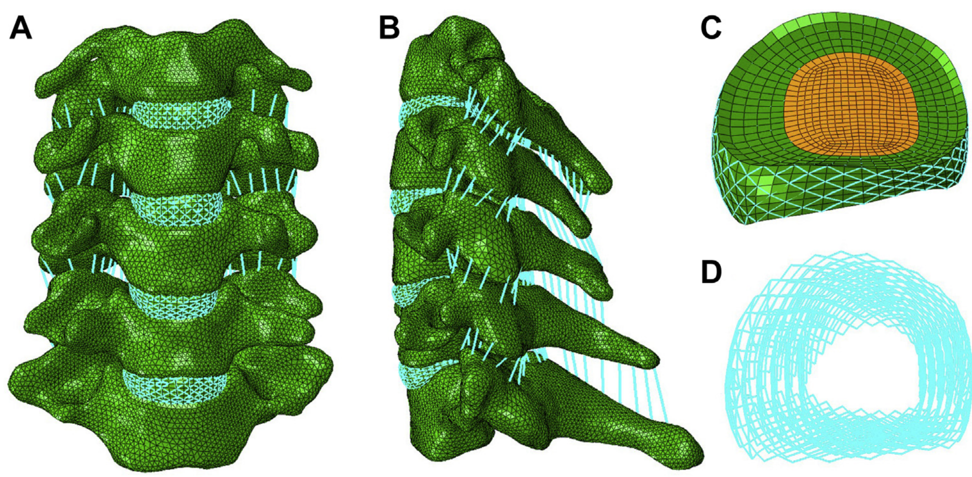

Figure 1. Finite element model of the intact C3-7 cervical spine: (**A**) front view, (**B**) sagittal view, (**C**) intact intervertebral disk, and (**D**) annulus fibers.

Table 1. Material Properties Assigned to the Finite Element Model

Component	Element Type	Young Modulus (MPa)	Poisson Ratio	Cross-Sectional Area (mm^2)
Cortical bone	C3D4	10,000	0.3	
Cancellous bone	C3D4	450	0.2	
Nucleus pulpous	C3D8H	Incompressible		
Annulus ground substance	C3D8H	4.2	0.45	
Annulus fibers	T3D2	450	0.3	
Anterior longitudinal	T3D2	Nonlinear*	0.3	6.1
Posterior longitudinal	T3D2	Nonlinear*	0.3	5.4
Ligamentum flavum	T3D2	Nonlinear*	0.3	50.1
Capsular	T3D2	Nonlinear*	0.3	46.6
Interspinous	T3D2	Nonlinear*	0.3	13.1
PEEK	C3D4	3760	0.3778	
Titanium alloy	C3D4	110,000	0.3	

PEEK, polyetheretherketone.
*Please refer to Figure 2 for details.

to further stabilize the surgical segment. The length and width of the plate were 52 and 17 mm, respectively. The length and diameter of the screw were 13 and 4 mm, respectively.

The corpectomies of C5 and C6 were simulated by removing the C4-5, C5-6, and C6-7 intervertebral disks; two thirds of the vertebral body in C5 and C6; and the corresponding anterior and posterior longitudinal ligaments. Figures 3B and E shows the FE model of ACCF using a conventional cage for interbody fusion. After the corpectomies, a conventional cage with a 12-mm diameter was trimmed into a suitable length and implanted into the intervertebral space. Because of the sharp, flat end, the cage had a point contact with the cortical end plates and left an obvious gap when contacting the oblique C7 superior end plate (Figure 3E, red arrow), which was consistent with the imaging features reported by previous publications.[14,16,18] The contact areas in the superior and inferior cage—end plate interfaces were only 0.28 and 0.13 cm^2, respectively.

Figures 3C and F shows the FE model of ACCF using the new cage for interbody fusion. After the corpectomies, a new cage with a 12-mm diameter was implanted into the space. Both ends of the cage were enlarged by adding a 2-mm-wide end ring to each end. The thickness of the end ring was 2 mm. Moreover, the ends were domed and angled to correctly match the corresponding end plates, consistent with the imaging features reported by previous publications.[16-18] Good matching between the end plate and cage was achieved using the Boolean calculation to remove the portion that overlapped with the vertebral body. The contact area in the cage—end plate interface was 0.63 cm^2, which was comparable with that in the previous multilevel ACDF construct. Similar to the surgical procedure in ACDF, both ACCF constructs were fixed by an anterior plate-screw system. For all surgical models, the interfaces at the cage—end plate and screw-bone were defined as a tied contact condition to simulate a complete fusion status.[21,22]

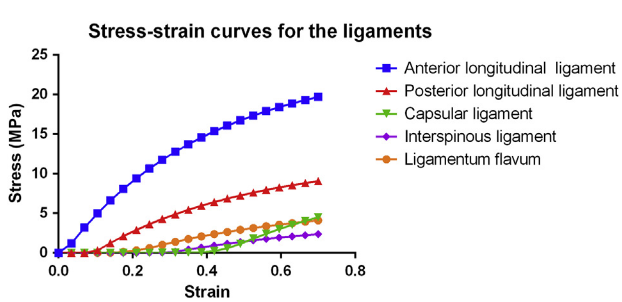

Figure 2. Ligament properties used for finite element modeling.

Loading and Boundary Conditions

For all FE models, the inferior surface of the C7 vertebra was constrained. Moment loads of 1.0 Nm were applied on the superior surface of the C3 vertebra to produce flexion, extension, bending, and rotation.[20,22,23] To validate the intact C3-7 FE model, the intersegmental ranges of motion (ROMs) and the load-displacement curves were compared with the outcomes of previous publications. The load-displacement curve was drawn by using the degrees of motion at moment loads of 0, 0.33, 0.67, and 1 Nm.[23,24] The surgical segment ROMs, end plate stresses, fixation system stresses, and screw-bone interfacial stresses were compared among the constructs of ACDF, ACCF using a conventional cage, and ACCF using the new cage.

RESULTS

Model Validation

The intersegmental ROMs at C3-4, C4-5, C5-6, and C6-7 were 3.58, 5.09, 5.58, and 5.03, respectively, in extension; 4.39, 5.64, 4.67,

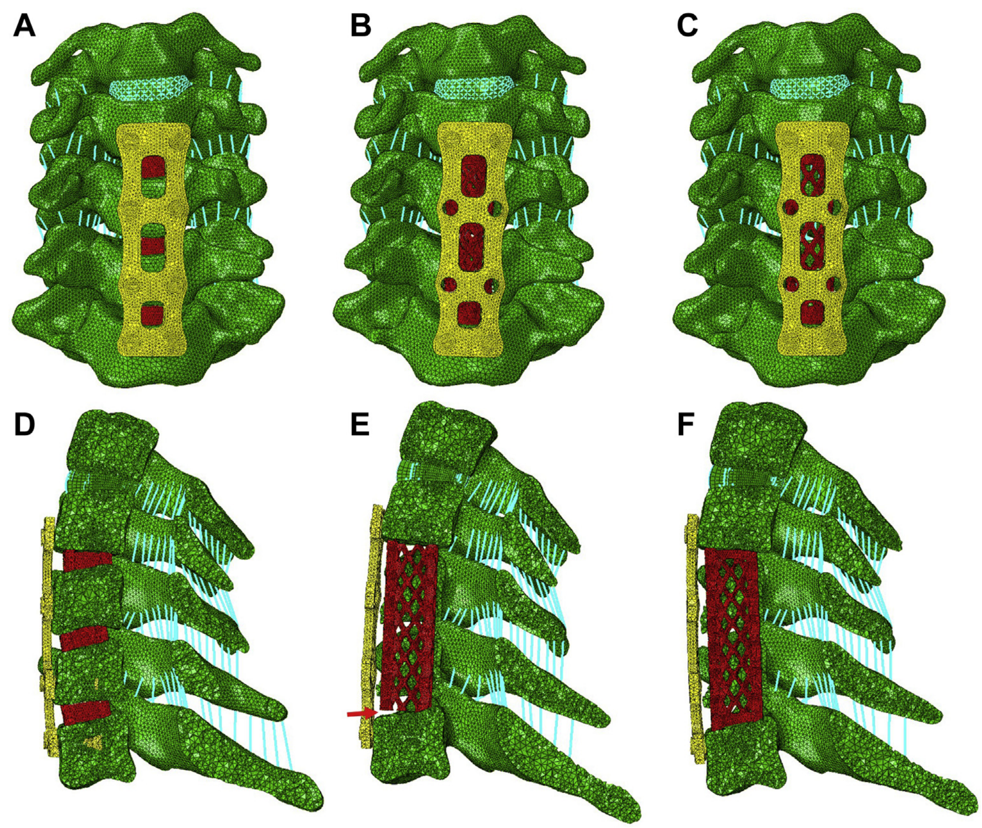

Figure 3. Finite element models of the surgical procedures: (**A**) front view of anterior cervical diskectomy and fusion (ACDF), (**B**) front view of anterior cervical corpectomy and fusion (ACCF) using the conventional cage, (**C**) front view of ACCF using the new cage, (**D**) sagittal view of ACDF, (**E**) sagittal view of ACCF using the conventional cage, and (**F**) sagittal view of ACCF using the new cage. The *red arrow* indicates the gap between the cage end and the C7 superior end plate.

and 4.68, respectively, in flexion; 3.2, 4.49, 2.97, and 2.1, respectively, in rotation; and 3.14, 3.47, 2.76, and 3.38, respectively, in bending. As shown in **Figure 4**, the intersegmental ROMs and the load-displacement curves in each motor direction showed good agreement with the outcomes of previous publications.

ROMs of the Surgical Constructs

As shown in **Figure 5A**, the ROMs of the intact C4-7 model in extension, flexion, rotation, and bending were 15.7, 15, 9.47, and 9.61, respectively. Postoperatively, the ROMs of ACDF, ACCF using a conventional cage, and ACCF using the new cage were significantly reduced to 0.47, 0.29, and 0.28, respectively, in extension; 0.47, 0.3, and 0.28, respectively, in flexion; 0.37, 0.33, and 0.24, respectively, in rotation; and 0.26, 0.31, and 0.28, respectively, in bending.

Cortical End Plate Stresses

Figure 5B shows the maximum von Mises stresses in the C7 superior end plates. The end plate stress peaks were the highest in the construct of ACCF using a conventional cage, wherein the stresses were 18.6, 18.6, 16.7, and 10.1 MPa in extension, flexion, rotation, and bending, respectively. In the same types of movement, the end plate stress peaks were significantly reduced by using the new cage for reconstruction in ACCF, which reduced to 14.3, 15.2, 8.4, and 7.7 MPa, respectively. The end plate stress peaks were the lowest in the construct of ACDF, wherein the stresses were 9.1, 9.1, 5.6, and 5.3 MPa, respectively, in the same types of movement. The stress distributions in the C7 superior end plates of the surgical constructs are shown in **Figure 6**.

Screw-Bone Interfacial Stresses

The maximum von Mises stresses in the screw-bone interfaces are shown in **Figure 5C**. In extension and flexion, the screw-bone interfacial stress peaks among the 3 constructs were quite similar, wherein the values ranged from 11.9 to 12.7 MPa. In rotation and bending, the screw-bone interfacial stresses in ACDF were 12.1 and 14.2 MPa, respectively, which were slightly higher than those in ACCF using a conventional cage (10.3 and 13.6 MPa,

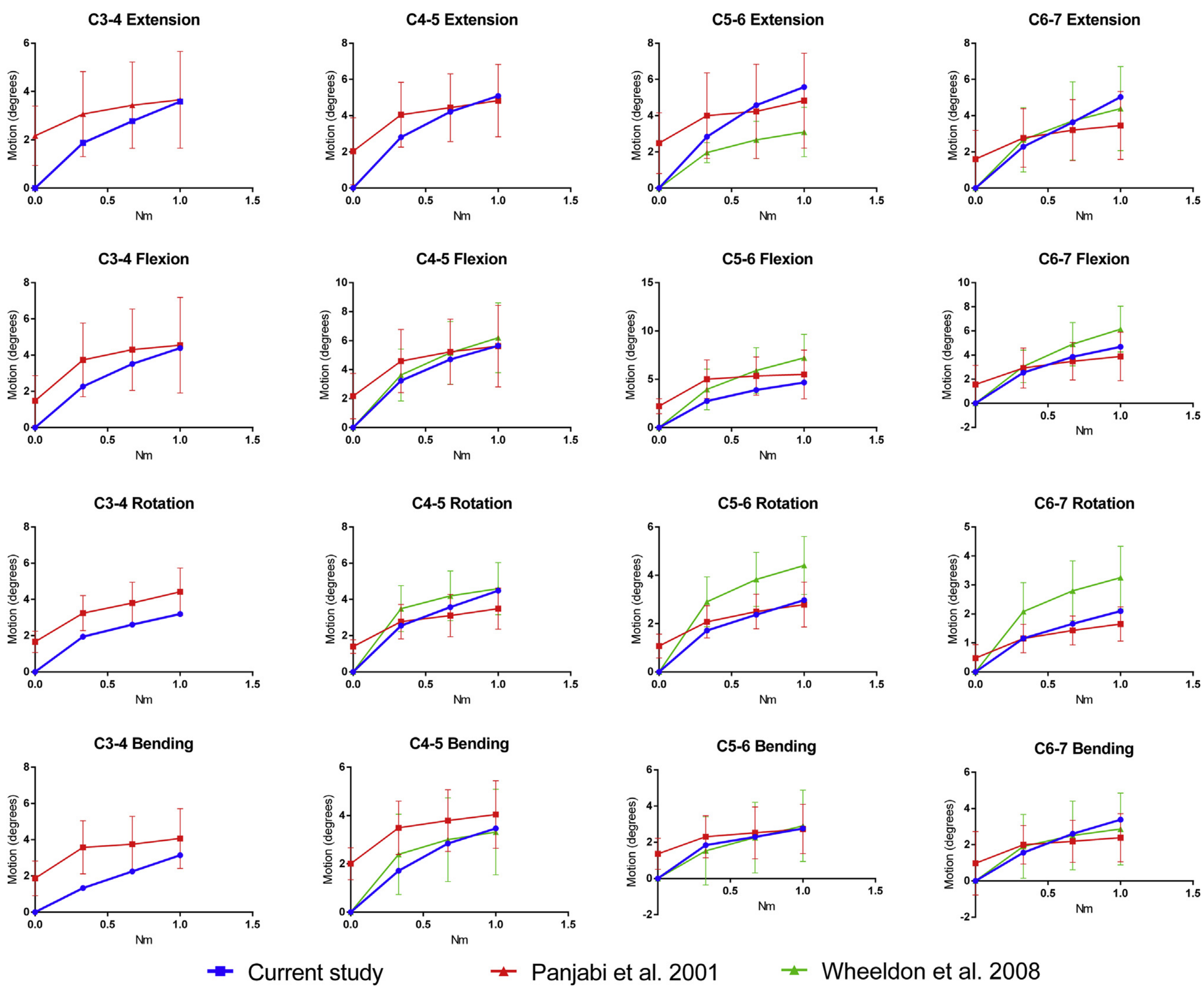

Figure 4. Comparison of the intersegmental load-displacement curves between the current intact finite element model and the outcomes of previous publications.

respectively) and those in ACCF using the new cage (9.7 and 12.6 MPa, respectively).

Fixation System Stresses

Figure 5D shows the maximum von Mises stresses of the fixation systems. The stress peaks of the fixation system in ACDF, ACCF using a conventional cage, and ACCF using the new cage were 32.5, 27.1, and 21.7 MPa, respectively, in extension; 32.5, 20.4, and 20.5 MPa, respectively, in flexion; 39.3, 26.1, and 18.6 MPa, respectively, in rotation; and 38.3, 31.7, and 25.7 MPa, respectively, in bending. The stress peaks of the fixation system were the highest in ACDF and the lowest in ACCF using the new cage. **Figure 7** shows the stress distributions in the screw-plate systems.

DISCUSSION

Construct Immobilization

This study comprehensively compared the biomechanical stabilities provided by multilevel ACCF and ACDF. Moreover, the effects of the new cage on the improvement of biomechanical performance in multilevel ACCF were assessed. As shown in the results, both ACDF and ACCF procedures could significantly reduce the ROMs; therefore, both ACDF and ACCF could achieve strong immobilization in the surgical segment. In all movement directions, the ROMs of the surgical segments decreased by 96.1%—98.2% postoperatively, which was consistent with the outcomes of previous publications.[10,25] Ouyang et al.[25] conducted an FE study to assess the biomechanical performance of ACCF and found

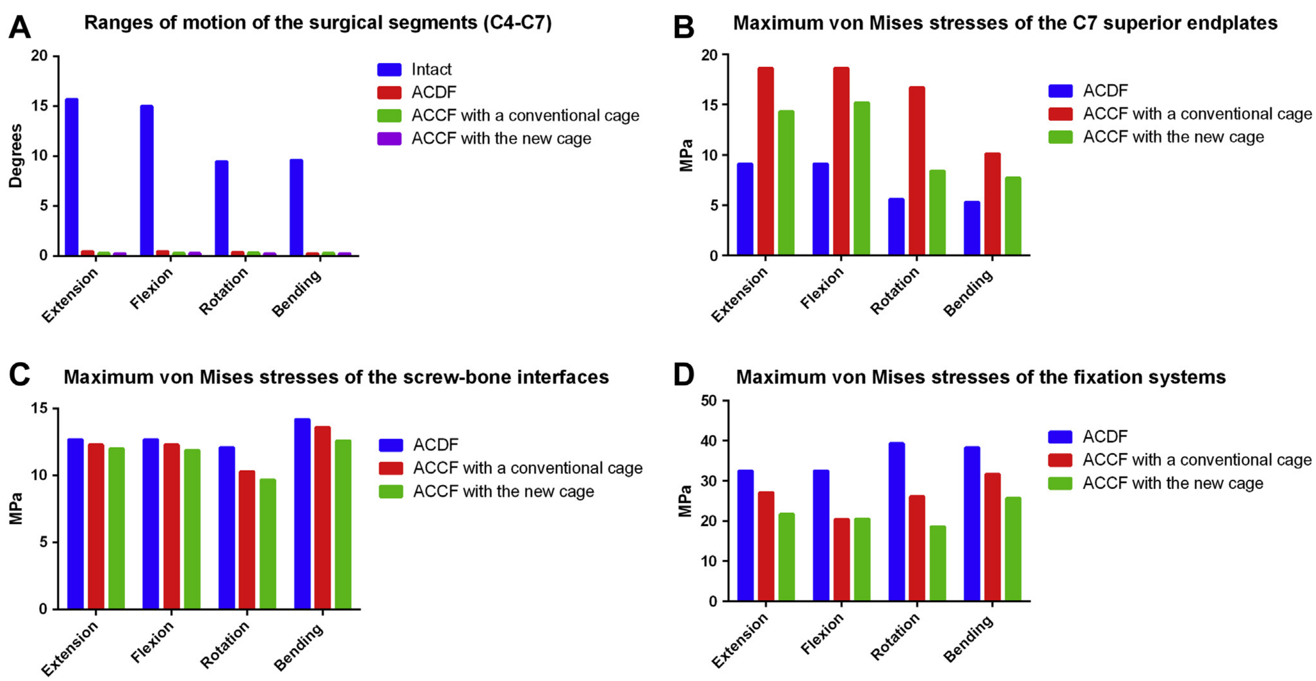

Figure 5. Comparisons of the (**A**) ranges of motion, (**B**) C7 superior cortical end plate stresses, (**C**) screw-bone interfacial stresses, and (**D**) fixation system stresses among the 3 surgical procedures. ACCF, anterior cervical corpectomy and fusion; ACDF, anterior cervical diskectomy and fusion.

that the ROM of the ACCF construct was 93%–96.8% less than that of the preoperative status. Oh et al.[10] retrospectively investigated the clinical and radiologic outcomes of using ACDF and ACCF to treat CSM. The outcomes also showed that both surgical procedures could reduce the ROMs of the surgical segments by approximately 70%.

Multiple studies have noted that the achievement of strong immobilization at the surgical segment is mainly attributed to the anterior fixation and interbody fusion.[26-28] In the early stage, anterior fixation offers an immediate fixation for the anterior column, which helps to decrease the cage subsidence rate and facilitate bony fusion.[29-31] Tsitsopoulos et al.[32] conducted a cadaveric study to compare the biomechanical stabilities provided via ACDF using a stand-alone cage and ACDF with an additional plate augmentation. Their outcomes showed that the intersegmental ROMs were reduced by only 49.2%–67.7% in the stand-alone cage group, whereas the placement of the screw-plate system significantly reduced the ROMs by 73.7%–92.8%.[32] In a similar cadaveric study conducted by Nayak et al.,[33] the outcomes also revealed that the segmental ROMs provided by the fixation system were 38.6%–79.3% less than those of the stand-alone cage group.

In the present study, the boundary conditions of the cage-bone interfaces were assigned to be tied contacts to simulate the status of bony fusion.[21,22] As a result of the bony fusion at the intervertebral space, the stiffness of the anterior column increases, which further enhances the stability of the construct. Li et al.[34] retrospectively analyzed the radiologic outcomes of 35 patients who underwent ACDF and found that the ROM of the treated level significantly decreased at any point in time after surgery. Compared with immediately after surgery, the ROMs of the treated level further reduced by 11.5% when the bony fusion was achieved at the intervertebral space.[34]

The results also showed that there were small differences in the ROMs of the surgical segment. The ROMs in the ACCF constructs were slightly less than those in the ACDF constructs, especially in ACCF using the new cage for reconstruction. The reason for this phenomenon may be that the stiffness of the anterior column is much greater in the ACCF construct since most of the anterior column consists of titanium alloy, which has a high elastic modulus.[19,21] Therefore, the anterior column of the ACDF construct was more prone to deform than that of the ACCF construct, which resulted in slightly greater ROMs.

Subsidence Resistance

Cage subsidence is a common postoperative complication in multilevel ACCF.[13-15] Although cage subsidence has few influences on the clinical outcomes in most patients, some severe cases may induce kyphosis, neurologic deterioration, and instrumental complications because of the substantial decrease in intervertebral height and the subsequent increase in stress load within the anterior plate.[13-15,35] Previous studies have found that ACCF induces a much higher cage subsidence rate than ACDF in the treatment of multilevel CSM.[36-38] Lin et al.[37] compared the outcomes of using ACCF and ACDF for treating multilevel CSM and found that the cage dislodgement and subsidence rate was

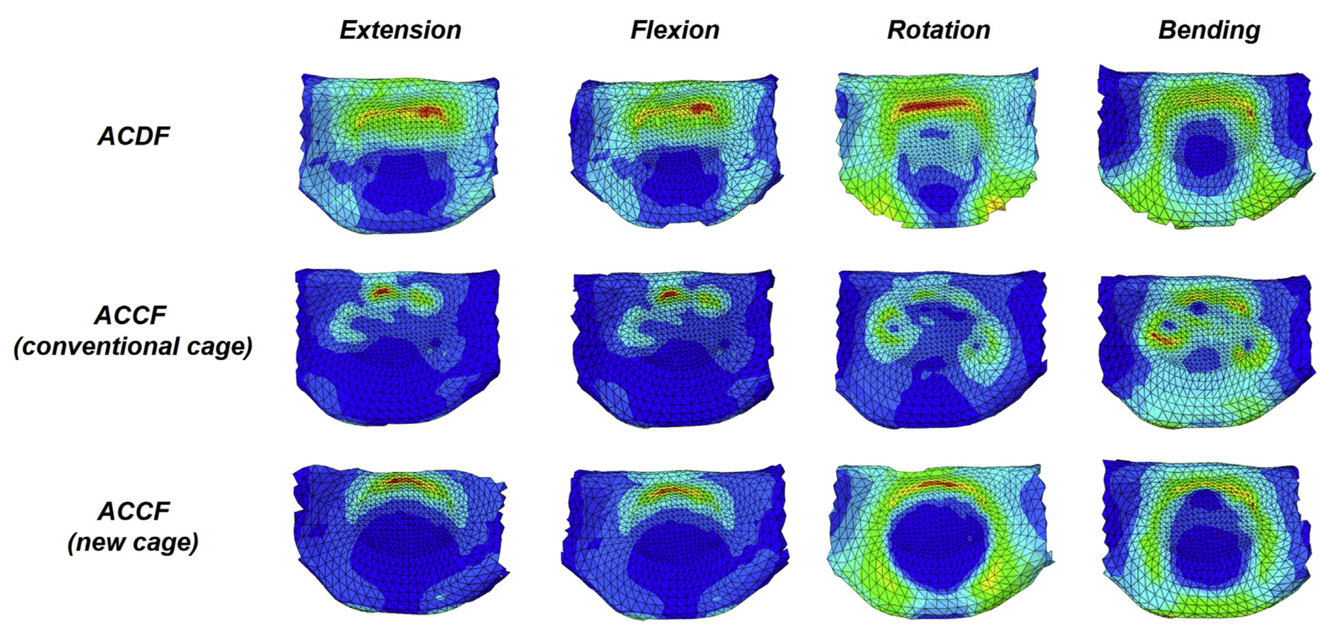

Figure 6. Stress distributions in the C7 superior cortical end plates. ACCF, anterior cervical corpectomy and fusion; ACDF, anterior cervical diskectomy and fusion.

9.5% in the ACCF group, whereas none of the patients in the ACDF group experienced cage dislodgement or subsidence. Guo et al.[38] reported that the rate of cage subsidence of using ACCF for the treatment of 3-level CSM was 12.5%. In addition, 1 patient experienced screw breakage because of cage subsidence.

The high interfacial stress concentration is an important factor that facilitates the cage penetrating into the end plate and inducing cage subsidence.[14,39,40] The outcomes of end plate stresses showed that multilevel ACCF using a conventional cage for vertebral body construction induced approximately 1-fold greater stress peaks on the end plate than multilevel ACDF (10.1–18.6 vs. 5.3–9.1 MPa,

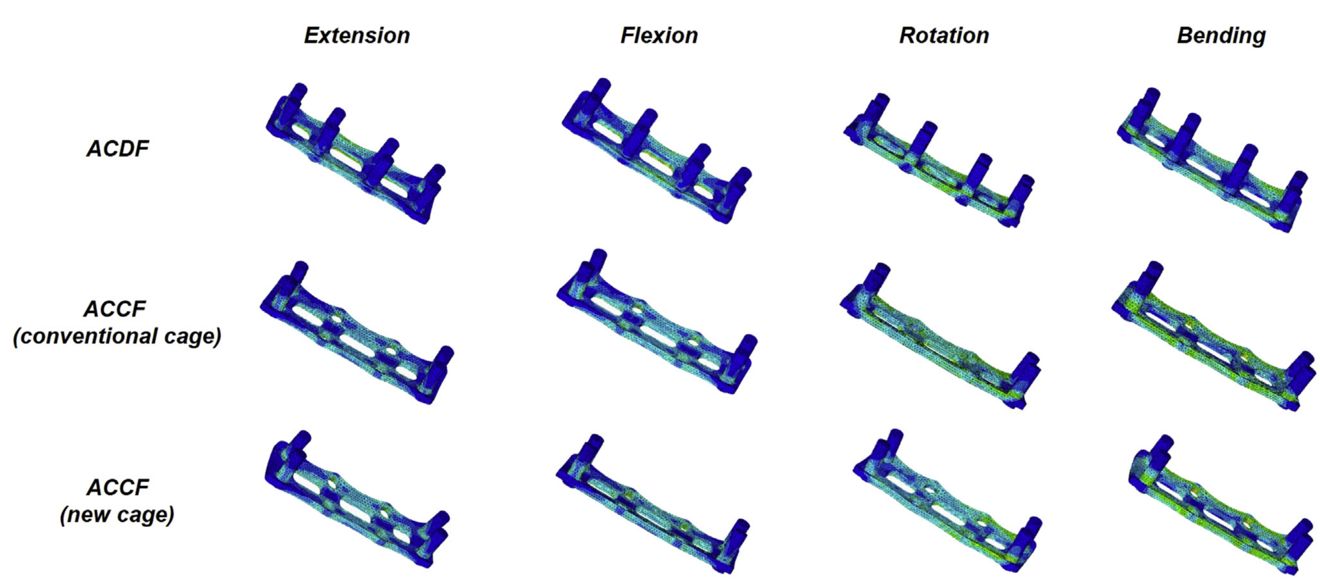

Figure 7. Stress distributions in the fixation systems. ACCF, anterior cervical corpectomy and fusion; ACDF, anterior cervical diskectomy and fusion.

respectively). Previous studies have noted that the fewer points for anterior screw fixation and the drawbacks of the conventional cage profile are the main implant-related factors that induce cage subsidence and subsequent instability.[14,40,41] For a conventional cage, the small footprints on the end and the geometric mismatching between the domed end plate and flat end substantially reduce the contact area with the end plate, which results in a large stress concentration and facilitates cage subsidence.[14,40,42]

To address these issues, some cages with new profiles have been reported to be used for vertebral body reconstruction in single-level ACCF.[16-18] By enlarging the surface area and simulating the end plate geometries in the cage end, these new cages offered much larger contact area with the end plate, which effectively alleviated the stress concentration and reduced the subsidence rate.[16-18] Lu et al.[39] performed a cadaveric study to assess the effects of the new cage profiles on the subsidence resistance in single-level ACCF. Compared with the conventional cage, the new cage end decreased the maximum load force on the end plate by 53.8%.[39] Although it is difficult to achieve 100% geometric matching with the end plates using the new cages with fixed profiles because the cervical geometry varies among patients,[42-44] the postoperative outcomes showed that these cages still exhibited close contact with the end plates and effectively reconstructed the intervertebral height and angle.[16-18] By simulating the end plate geometry, these new cages significantly decreased the interval between the cage end and the end plate compared with conventional corpectomy cages with a flat end.[17,18] Therefore, the disappearance of the interval only leads to a slight subsidence of the cage footprint that initially contacts the end plate. The integrity and mechanical strength of the end plate are not obviously influenced.[45,46] Additionally, the disappearance of the interval results in a significant increase in the contact area, which further alleviates the stress concentration at the interface and decreases the risk of postoperative subsidence.[47,48]

Although much higher compressive and torque loads are applied to the construct as the fusion level increases,[40] the outcomes of the end plate stresses showed that, compared with ACCF using a conventional cage, the use of the new cage in multilevel ACCF still decreased the stress peaks on the end plate by 23%—50%. As shown in the end plate stress nephograms, the stress distribution in ACCF using a conventional cage mainly focused on the posterior part of the end plate because of the limited contact area at the interface. By using the new cage in ACCF, the contact area at the cage—end plate effectively expanded, and the stress distribution on the end plate became homogeneous, which alleviated the concentration of stress and decreased the risk of cage subsidence.[16,39]

Although the end surface areas of the new ACCF cage and the ACDF cage were similar, the stress peak in the ACDF end plate was still lower than that in ACCF by 31.2%—40.1%. The reason for the superiority of subsidence resistance in the ACDF construct may also be that the stiffness of the anterior column was much lower because of the reservation of the vertebral bodies.[19,21] Compared with ACCF, more loads from the skull were shared by the fixation system in ACDF, and the stress load at the cage-bone interface correspondingly decreased,[49] which resulted in much lower stress peaks in the end plate and helped to further decrease the risk of cage subsidence.[16,39]

Risks of Instrument-Related Complications

Among the 3 constructs, ACCF using the new cage for reconstruction induced the lowest stress peaks in the screw-bone interfaces and anterior screw-plate system, especially in rotation and bending. The decrease in the stress load at the interface and anterior instrument alleviated the fatigues of the fixation and interfaces, which helps to decrease the risks of screw looseness, screw breakage, and plate extrusion.[22] Compared with the use of a conventional cage, the reasons for the lower stress loads at the fixation system and screw-bone interface by implanting the new cage were attributed to the increase in the contact area at the cage—end plate interface, which provided greater capacity to stabilize the anterior column.[16,18,39] Therefore, the fixation system produced less bearing and sharing loads to resist the movements of the surgical segments. The ACDF construct induced the highest stress peaks in the fixation system and screw-bone interface because the stiffness of the anterior column was much lower than that in the ACCF construct.[19,21] Therefore, the anterior column was more prone to deform in the ACDF construct, which resulted in the fixation system yielding more loads to stabilize the construct.

However, once cage subsidence occurred in the ACCF constructs, the stress loads on the screw-bone interface and fixation system significantly increased.[50] Clinical outcomes of previous publications showed that instrument-related complications were more likely to occur in ACCF using the conventional cage for construction because of the high incidence of cage subsidence.[37,38,40] The loss of integrity of the cortical end plate caused by cage subsidence reduced the stiffness and stability of the anterior column, which conversely increased the stress loads on the fixation system and the screw-bone interface.[50] Compared with the conventional cage, the use of the new cage for reconstruction in multilevel ACCF effectively reduced the stress peaks at the cage—end plate interface because of the advantageous design profiles,[16,39] which helped to prevent cage subsidence to maintain the biomechanical stability of the surgical construct and decrease the risks of instrument-related complications in ACCF.[16,39]

Limitations

This study has several limitations. The degrees of disk degeneration and facet arthropathy are difficult to simulate in the FE model.[51] In this study, FE modeling of the intact cervical spine was based on the CT data of a young healthy man, which might neglect the influence of degenerative pathologies on the biomechanical performance of the cervical spine. However, we suggest that these influences would have little effect on the results because the disk was removed after decompression, and the facet arthropathy had a limited impact on the stability of the surgical constructs. In addition, the results of the multilevel ACDF and ACCF procedures were based on a single FE model. The biomechanical characteristics of this FE model may not be analogous to the situation of the cervical spine during severe pathologic changes, such as severe osteoporosis and cervical kyphosis, which significantly decrease the mechanical strength of the vertebral body and change the kinematics of the involved level, respectively.[52,53] Further studies are needed to analyze these specific situations.

CONCLUSIONS

The application of the new cage that possessed enlarged ends and emulated the end plate geometries can effectively decrease the risks of cage subsidence and instrument-related complications in multilevel ACCF. Under the condition where cage subsidence was prevented, ACCF was superior to ACDF in terms of construct stability and avoiding instrument-related complications.

REFERENCES

1. Toledano M, Bartleson JD. Cervical spondylotic myelopathy. *Neurol Clin*. 2013;31:287-305.

2. Mummaneni PV, Kaiser MG, Matz PG, et al. Cervical surgical techniques for the treatment of cervical spondylotic myelopathy. *J Neurosurg Spine*. 2009;11:130-141.

3. Liu J, Chen X, Liu Z, Long X, Huang S, Shu Y. Anterior cervical discectomy and fusion versus corpectomy and fusion in treating two-level adjacent cervical spondylotic myelopathy: a minimum 5-year follow-up study. *Arch Orthop Trauma Surg*. 2015;135:149-153.

4. Burkhardt JK, Mannion AF, Marbacher S, et al. A comparative effectiveness study of patient-rated and radiographic outcome after 2 types of decompression with fusion for spondylotic myelopathy: anterior cervical discectomy versus corpectomy. *Neurosurg Focus*. 2013;35:E4.

5. Lau D, Chou D, Mummaneni PV. Two-level corpectomy versus three-level discectomy for cervical spondylotic myelopathy: a comparison of perioperative, radiographic, and clinical outcomes. *J Neurosurg Spine*. 2015;23:280-289.

6. Han YC, Liu ZQ, Wang SJ, Li LJ, Tan J. Is anterior cervical discectomy and fusion superior to corpectomy and fusion for treatment of multilevel cervical spondylotic myelopathy? A systemic review and meta-analysis. *PLoS One*. 2014;9:e87191.

7. Xiao SW, Jiang H, Yang LJ, Xiao ZM. Anterior cervical discectomy versus corpectomy for multilevel cervical spondylotic myelopathy: a meta-analysis. *Eur Spine J*. 2015;24:31-39.

8. Jiang SD, Jiang LS, Dai LY. Anterior cervical discectomy and fusion versus anterior cervical corpectomy and fusion for multilevel cervical spondylosis: a systematic review. *Arch Orthop Trauma Surg*. 2012;132:155-161.

9. Fountas KN, Kapsalaki EZ, Nikolakakos LG, et al. Anterior cervical discectomy and fusion associated complications. *Spine (Phila Pa 1976)*. 2007;32:2310-2317.

10. Oh MC, Zhang HY, Park JY, Kim KS. Two-level anterior cervical discectomy versus one-level corpectomy in cervical spondylotic myelopathy. *Spine (Phila Pa 1976)*. 2009;34:692-696.

11. Wei L, Cao P, Xu C, et al. Comparison of three anterior techniques in the surgical treatment of three-level cervical spondylotic myelopathy with intramedullary T2-weighted increased signal intensity. *World Neurosurg*. 2019;126:e842-e852.

12. Hartmann S, Tschugg A, Obernauer J, Neururer S, Petr O, Thome C. Cervical corpectomies: results of a survey and review of the literature on diagnosis, indications, and surgical technique. *Acta Neurochir (Wien)*. 2016;158:1859-1867.

13. Daubs MD. Early failures following cervical corpectomy reconstruction with titanium mesh cages and anterior plating. *Spine (Phila Pa 1976)*. 2005;30:1402-1406.

14. Wu J, Luo D, Ye X, Luo X, Yan L, Qian H. Anatomy-related risk factors for the subsidence of titanium mesh cage in cervical reconstruction after one-level corpectomy. *Int J Clin Exp Med*. 2015;8:7405-7411.

15. Bilbao G, Duart M, Aurrecoechea JJ, et al. Surgical results and complications in a series of 71 consecutive cervical spondylotic corpectomies. *Acta Neurochir (Wien)*. 2010;152:1155-1163.

16. Lu T, Liu C, Yang B, et al. Single-level anterior cervical corpectomy and fusion using a new 3D-printed anatomy-adaptive titanium mesh cage for treatment of cervical spondylotic myelopathy and ossification of the posterior longitudinal ligament: a retrospective case series study. *Med Sci Monit*. 2017;23:3105-3114.

17. Zhang Y, Quan Z, Zhao Z, et al. Evaluation of anterior cervical reconstruction with titanium mesh cages versus nano-hydroxyapatite/polyamide66 cages after 1- or 2-level corpectomy for multilevel cervical spondylotic myelopathy: a retrospective study of 117 patients. *PLoS One*. 2014;9:e96265.

18. Fengbin Y, Jinhao M, Xinyuan L, Xinwei W, Yu C, Deyu C. Evaluation of a new type of titanium mesh cage versus the traditional titanium mesh cage for single-level, anterior cervical corpectomy and fusion. *Eur Spine J*. 2013;22:2891-2896.

19. Kallemeyn N, Gandhi A, Kode S, Shivanna K, Smucker J, Grosland N. Validation of a C2-C7 cervical spine finite element model using specimen-specific flexibility data. *Med Eng Phys*. 2010;32:482-489.

20. Chen WM, Jin J, Park T, Ryu KS, Lee SJ. Strain behavior of malaligned cervical spine implanted with metal-on-polyethylene, metal-on-metal, and elastomeric artificial disc prostheses - a finite element analysis. *Clin Biomech (Bristol, Avon)*. 2018;59:19-26.

21. Wu TK, Meng Y, Wang BY, et al. Biomechanics following skip-level cervical disc arthroplasty versus skip-level cervical discectomy and fusion: a finite element-based study. *BMC Musculoskelet Disord*. 2019;20:49.

22. Zhao L, Chen J, Liu J, et al. Biomechanical analysis on of anterior transpedicular screw-fixation after two-level cervical corpectomy using finite element method. *Clin Biomech (Bristol, Avon)*. 2018;60:76-82.

23. Panjabi MM, Crisco JJ, Vasavada A, et al. Mechanical properties of the human cervical spine as shown by three-dimensional load-displacement curves. *Spine (Phila Pa 1976)*. 2001;26:2692-2700.

24. Wheeldon JA, Stemper BD, Yoganandan N, Pintar FA. Validation of a finite element model of the young normal lower cervical spine. *Ann Biomed Eng*. 2008;36:1458-1469.

25. Ouyang P, Lu T, He X, Gao Z, Cai X, Jin Z. Biomechanical comparison of integrated fixation cage versus anterior cervical plate and cage in anterior cervical corpectomy and fusion (ACCF): a finite element analysis. *Med Sci Monit*. 2019;25:1489-1498.

26. Gao R, Yang L, Chen H, Liu Y, Liang L, Yuan W. Long term results of anterior corpectomy and fusion for cervical spondylotic myelopathy. *PLoS One*. 2012;7:e34811.

27. Song KJ, Choi BY. Current concepts of anterior cervical discectomy and fusion: a review of literature. *Asian Spine J*. 2014;8:531-539.

28. Wang JC, McDonough PW, Endow KK, Delamarter RB. Increased fusion rates with cervical plating for two-level anterior cervical discectomy and fusion. *Spine (Phila Pa 1976)*. 2000;25:41-45.

29. Song KJ, Kim GH, Choi BY. Efficacy of PEEK cages and plate augmentation in three-level anterior cervical fusion of elderly patients. *Clin Orthop Surg*. 2011;3:9-15.

30. Song KJ, Taghavi CE, Lee KB, Song JH, Eun JP. The efficacy of plate construct augmentation versus cage alone in anterior cervical fusion. *Spine (Phila Pa 1976)*. 2009;34:2886-2892.

31. Oliver JD, Goncalves S, Kerezoudis P, et al. Comparison of outcomes for anterior cervical discectomy and fusion with and without anterior plate fixation: a systematic review and meta-analysis. *Spine (Phila Pa 1976)*. 2018;43:E413-E422.

32. Tsitsopoulos PP, Voronov LI, Zindrick MR, et al. Biomechanical stability analysis of a stand-alone cage, static and rotational-dynamic plate in a two-level cervical fusion construct. *Orthop Surg*. 2017;9:290-295.

33. Nayak AN, Stein MI, James CR, et al. Biomechanical analysis of an interbody cage with three integrated cancellous lag screws in a two-level cervical spine fusion construct: an in vitro study. *Spine J*. 2014;14:3002-3010.

34. Li Z, Wu H, Chu J, et al. Motion analysis of dynamic cervical implant stabilization versus anterior discectomy and fusion: a retrospective analysis of 70 cases. *Eur Spine J*. 2018;27:2772-2780.

35. Takase H, Murata H, Sato M, et al. Delayed C5 palsy after anterior cervical decompression surgery: preoperative foraminal stenosis and postoperative spinal cord shift increase the risk of palsy. *World Neurosurg*. 2018;120:e1107-e1119.

36. Li Z, Huang J, Zhang Z, Li F, Hou T, Hou S. A comparison of multilevel anterior cervical

discectomy and corpectomy in patients with 4-level cervical spondylotic myelopathy: a minimum 2-year follow-up study: multilevel anterior cervical discectomy. *Clin Spine Surg*. 2017;30:E540-E546.

37. Lin Q, Zhou X, Wang X, Cao P, Tsai N, Yuan W. A comparison of anterior cervical discectomy and corpectomy in patients with multilevel cervical spondylotic myelopathy. *Eur Spine J*. 2012;21:474-481.

38. Guo Q, Bi X, Ni B, et al. Outcomes of three anterior decompression and fusion techniques in the treatment of three-level cervical spondylosis. *Eur Spine J*. 2011;20:1539-1544.

39. Lu T, Liang H, Liu C, et al. Effects of titanium mesh cage end structures on the compressive load at the endplate interface: a cadaveric biomechanical study. *Med Sci Monit*. 2017;23:2863-2870.

40. Chen Y, Chen D, Guo Y, et al. Subsidence of titanium mesh cage: a study based on 300 cases. *J Spinal Disord Tech*. 2008;21:489-492.

41. Wang JC, Hart RA, Emery SE, Bohlman HH. Graft migration or displacement after multilevel cervical corpectomy and strut grafting. *Spine (Phila Pa 1976)*. 2003;28:1016-1021 [discussion: 1021-1022].

42. Lou J, Liu H, Rong X, Li H, Wang B, Gong Q. Geometry of inferior endplates of the cervical spine. *Clin Neurol Neurosurg*. 2016;142:132-136.

43. Feng H, Fang X, Huang D, Yu C, Zhao S, Hao D. Quantitative morphometric study of the subaxial cervical vertebrae end plate. *Spine J*. 2017;17:269-276.

44. Feng H, Fang X-Y, Huang D-G, et al. A morphometric study of the middle and lower cervical vertebral endplates and their components. *Medicine*. 2017;96:e6296.

45. Pitzen T, Schmitz B, Georg T, et al. Variation of endplate thickness in the cervical spine. *Eur Spine J*. 2004;13:235-240.

46. Schmitz B, Pitzen T, Beuter T, Steudel WI, Reith W. Regional variations in the thickness of cervical spine endplates as measured by computed tomography. *Acta Radiol*. 2004;45:53-58.

47. Lowe TG, Hashim S, Wilson LA, et al. A biomechanical study of regional endplate strength and cage morphology as it relates to structural interbody support. *Spine (Phila Pa 1976)*. 2004;29:2389-2394.

48. Ordway NR, Rim BC, Tan R, Hickman R, Fayyazi AH. Anterior cervical interbody constructs: effect of a repetitive compressive force on the endplate. *J Orthop Res*. 2012;30:587-592.

49. Peterson JM, Chlebek C, Clough AM, et al. Stiffness matters: part II-the effects of plate stiffness on load-sharing and the progression of fusion following anterior cervical discectomy and fusion in vivo. *Spine (Phila Pa 1976)*. 2018;43:E1069-E1076.

50. Colman MW, Guss A, Bachus KN, Spiker WR, Lawrence BD, Brodke DS. Fixed-angle, posteriorly connected anterior cage reconstruction improves stiffness and decreases cancellous subsidence in a spondylectomy model. *Spine (Phila Pa 1976)*. 2016;41:E519-E523.

51. Guo LX, Yin JY. Finite element analysis and design of an interspinous device using topology optimization. *Med Biol Eng Comput*. 2019;57:89-98.

52. Ordway NR, Lu Y-M, Zhang X, Cheng C-C, Fang H, Fayyazi AH. Correlation of cervical endplate strength with CT measured subchondral bone density. *Eur Spine J*. 2007;16:2104-2109.

53. Ruangchainikom M, Daubs MD, Suzuki A, et al. Effect of cervical kyphotic deformity type on the motion characteristics and dynamic spinal cord compression. *Spine (Phila Pa 1976)*. 2014;39:932-938.

Conflict of interest statement: This work was supported by the National Natural Science Foundation of China (81571209).

Received 21 March 2019; accepted 4 May 2019

Citation: World Neurosurg. (2019) 129:e87-e96.
https://doi.org/10.1016/j.wneu.2019.05.037

Journal homepage: ***www.journals.elsevier.com/world-neurosurgery***

Available online: ***www.sciencedirect.com***

1878-8750/$ - see front matter